INTERNATIONAL JOURNAL OF ENGINEERING MANAGEMENT SCIENCE
journal homepage: www.ijems.online/index.php/ijems/index

Synthesis of Millstone Novel Schiff Base and Its Transition Metal Complexes: Characterization and Study of Its Biological Activity

Kapil Totawar[1], L. P. Shinde[2], Anil Shinde[3*]

[1,2] Department of Chemistry NES Science College, Nanded (MS)
[3]MJPV Arts, Commerce & Shri VKK Science College Dhadagon (MS)

Received: 5-5-2026 ***Revised: 18-6-2026*** ***Accepted: 22-6-2026***

Keyword	***Abstract***
Nonlinear Optical Characteristics, Metal Complexes, Antibacterial Action, Anticancer Activity, Schiff Bases.	Primary amines containing carbonyl groups condense to form Schiff bases, which are adaptable ligands. Because of their diverse range of biological activity, these chemicals are highly significant in the domains of medicine and pharmacology. The majority of them exhibit biological properties like antifungal, antibacterial, and anticancer action. Numerous studies have been conducted on transition metal complexes having biological activity that are generated from Schiff base ligands. The synthesis and biological activity of Schiff bases and their transition complexes are summed up here.

1. Interdiction:

Schiff bases and their transition metal complexes have diverse applications, serving as models for metal biosites and metalloenzyme reaction centers, as well as finding use in nonlinear optics, catalysis of organic reactions (including asymmetric synthesis), and luminescent materials[1-5]. Beyond these applications, they exhibit a variety of biological activities, functioning as anticancer, antifungal, antibacterial, antiviral, and antiparasitic agents. Schiff base complexes, particularly those with transition metals, have demonstrated significant potential in inhibiting the growth of pathogenic microorganisms, especially bacteria and fungi[6]. Nitrogen-containing aromatic heterocyclic Schiff bases and their transition complexes can strongly interact with biomacromolecules. Transition metals like copper, nickel and cobalt play crucial roles in medicinal chemistry, forming complexes with various ligands and participating in biological redox processes. Complexation often enhances the activity of the ligand. Copper, an important trace element, is involved in numerous biological processes. Copper complexes have been widely studied for their ability to cleave DNA, a property relevant to cancer treatment, by generating reactive oxygen species[7].Tetra-azonmacrocyclic copper complexes have demonstrated anti-HIV activity. Furthermore, copper's tendency to accumulate in tumors due to selective cancer cell membrane permeability has led to the screening of numerous copper complexes for anticancer activity, with some showing promise in both in vitro and invivo studies [8]. Developing compounds with both antioxidant properties and strong DNA-binding is crucial for operative cancer therapy and copper complexes have shown significant potential in this area.

Cobalt, a trace element essential for human health (as a component of vitamin B12, crucial for iron metabolism and hemoglobin synthesis), can be detrimental in excess, causing various health issues including cardiovascular, renal, and neurological

problems. Conversely, cobalt deficiency can lead to growth retardation, anemia, and weight loss. Schiff bases are being explored for cobalt sensing applications, and a cobalt(III) complex, Doxovir, has reached phase-II antiviral clinical trials, highlighting the potential of cobalt-based metallo drugs. Given cobalt's relative safety compared to platinum, this review summarizes the synthesis, structure, and anticancer properties of cobalt (III)

and (II) Schiff base complexes, aiming to correlate their biochemical and biophysical properties to facilitate the design of more effective anticancer agents[9

Nickel, while essential in trace amounts for various biological functions, particularly within specific enzymes, remains an element whose biochemical activity is not fully understood[10]. Nickel(II) Schiff base complexes, especially those incorporating sulphur donors, are of particular interest due to the prevalence of sulphur-rich coordination environments in biological nickel centers. These centers are found in enzymes like ureases, methyl-S-coenzyme-M-methyl reductase and hydrogenases[11].
Nickel's known biological activities are diverse, encompassing antiepileptic, vitamin-like, antibacterial, antifungal, antimicrobial, and anticancer/antiproliferative effects. The interaction of DNA with mononuclear nickel(II) complexes has also been documented[12]. The broader study of nickel complexes with multidentate Schiff base ligands is significant in redox enzyme systems, bioinorganic chemistry and as potential models for biological active sites or catalytic agents [13].
This study focuses on the preparation and characterization of novel complexes of metal derived from a newly synthesized Schiff base ligand. The ligand, 2-(3-(trifluoromethyl)phenylimino)methyl)-5-methoxyphenol (TFPMMP-SB5), was prepared through the heatimg of 3-(trifluoromethyl)benzenamine with 2-hydroxy-4-methoxybenzaldehyde. Subsequently, this Schiff base ligand was reacted with a variety of metal salts to yield the corresponding metal complexes. The resulting compounds were characterized using a range of techniques, including physical properties such as color and melting point, as well as spectroscopic analyses such as 1H NMR, IR, UV-Vis, magnetic susceptibility measurements, ESR, XRD, and TGA. These spectral data were utilized to elucidate the molecular structures of both the ligand and the synthesized metal complexes. Furthermore, the biological activity of these compounds was investigated against Gram-positive bacterial strains Bacillus subtilis and Staphylococcus aureus, and Gram-negative bacterial strains Escherichia coli and Klebsiellapneumoniae.

2. Materials and Methods:

Chemicals:
The chemicals used in this study included salicylaldehyde (Merck, AR grade), ethanol (Merck, AR grade), cobalt(II) chloride dihydrate (Sigma Aldrich), nickel(II) chloride hexahydrate (Sigma Aldrich), copper(II) chloride dihydrate (Sigma Aldrich), and manganese(II) chloride tetrahydrate (Sigma Aldrich).
Apparatus:
Borosilicate glassware was used throughout the experiments. Analytical balance unit for weighing samples exceeding 50 mg. For samples weighing less than 50 mg, a semi-micro balance was utilized.
The Schiff base ligand, 2-(3-(trifluoromethyl)phenyl)imino)methyl)-5-methoxyphenol (Fig 1.1), was prepared by the equimolar condensation of 3-(trifluoromethyl)benzenamine with 2-hydroxy-4-methoxybenzaldehyde. Briefly, salicyldehyde (0.01 mole) in 10 mL of ethanol was added to a stirred ethanolic solution (10 mL) of the amine (0.01 mole). The resulting mixture was refluxed for 2-3 hours. Upon cooling, a precipitate formed immediately. This precipitate was then collected by filtration, washed with ethanol, and subsequently dried. Recrystallization of the crude product from aqueous ethanol afforded the pure product in 78% yield. The synthetic route for the Schiff base is depicted in Figure 1.1.

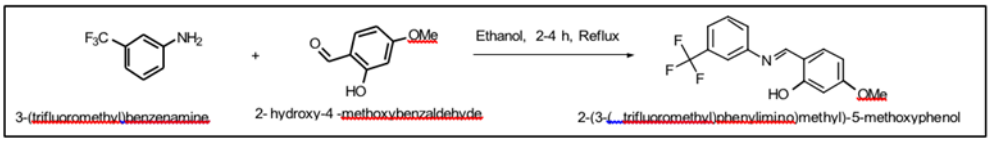

Fig 1.1: Preparation of Ligand (TFPMMP-SB5)

Equimolar solutions of the ligand and the respective metal chloride salts (Ni(II), Cu(II), Co(II) and Mn(II)) were prepared in ethanol at a 2:1 ligand-to-metal molar ratio. These mixtures were then heated in a water bath for 2-3 hrs. Following heating, the reaction mixtures were cooled, resulting in the precipitation of colored solids. These solids were subsequently collected by filtration, thoroughly washed with ethanol to remove any unreacted starting materials, and then dried under vacuum. This general synthetic procedure was consistently used for all the metal complexes.
Characterization of the Schiff base ligand and its metal complexes involved various spectroscopic and analytical techniques, including UV-Visible, PMR, IR, XRD, ESR, magnetic susceptibility measurements, and TGA. The

elemental analysis (C, H, N) of the compounds was carried out on a Perkin Elmer 240 C (USA) elemental analyzer, Melting points of compounds were determined with open glass capillary tubes on a Polmon instrument (model No. MP-96). NMR spectra of all the synthesized ligands were recorded in CDCl3 / Deuterated DMSO using TMS as an internal standard reference on a Bruker 400 MHz spectrometer. Vibrational Infrared spectra of the ligand and the metal complexes were recorded in the range of 4000-400 cm−1 using a Shimadzu IR Prestige-21 spectrophotometer from KBr discs. Electronic spectra of the complexes were recorded on a Shimadzu UV-Vis 2600 spectrophotometer in the wavelength range of 200-800 nm using DMSO as solvent. The thermo gravimetric analysis was carried out in dynamic nitrogen atmosphere with a heating rate of 10oC min−1 using Mettler Toledo Star system in the temperature range of 30-1000oC. EPR spectra of the Cu (II) complexes were recorded using JES-FA 200 ESR spectrometer (JEOL-Japan) at liquid nitrogen temperature (77K).

3. Physical Parameters:

The Schiff base described herein represents a novel compound, synthesized for the first time via a condensation reaction between the corresponding amine and aldehyde, yielding a crystalline solid. The resulting transition metal complexes exhibit distinct bright colors and are non-hygroscopic. These complexes demonstrate insolubility in water but exhibit complete solubility in DMSO at ambient temperature. Furthermore, all synthesized metal complexes demonstrate significant thermal stability. Comprehensive physical parameters and spectral data for both the ligand and the synthesized metal complexes are detailed in the tables presented below (Table 1.1).

Table 1.1: Physical parameters of (TFPMMP-SB5) and its complexes

S.No	Compound	Color	Yield (%)	MP
1	TFPMMP-SB5	Light cream	85	182
2	$(TFPMMP\text{-}SB5)_2$ Cu	Cream	68	270
3	$(TFPMMP\text{-}SB5)_2$ Ni	buff	80	275
4	$(TFPMMP\text{-}SB5)_2$ Co	green	76	290
5	$(TFPMMP\text{-}SB5)_2$ $(H_2O)_2$ Mn	Dark Brown	72	285

II. Elemental Analysis of TFPMDMP-SB5 and its Metal Complexes

Table 1.2: Elemental Analysis of (TFPMMP-SB5) and its complexes

S.No	Compound	Molecular formula	Mw	Elemental analysis Observed (Calculated)			
				% C	% H	% N	% M
1	TFPMMP-SB5	$C_{15}H_{12}F_3NO_2$	295.08	60.92 (61.02)	3.90 (4.10)	4.64 (4.74)	
2	$(TFPMMP\text{-}SB35)_2$ Cu	$C_{28}H_{18}CuF_6N_2O_2$	651.08	55.11 (55.26)	3.36 (3.40)	4.13 (4.30)	9.62 (9.75)
3	$(TFPMMP\text{-}SB5)_2$ Ni	$C_{30}H_{22}F_6N_2NiO_4$	646.08	55.57 (55.67)	3.33 (3.43)	4.13 (4.33)	8.93 (9.07)
4	$(TFPMMP\text{-}SB5)_2$ Co	$C_{30}H_{22}CoF_6N_2O_4$	647.08	55.55 (55.65)	3.33 (3.43)	4.22 (4.33)	8.92 (9.10)
5	$(TFPMMP\text{-}SB5)_2$ $(H_2O)_2$ Mn	$C_{31}H_{29}F_6MnN_2O_6$	694.13	53.51 (53.61)	3.99 (4.03)	3.93 (4.03)	7.81 (7.91)

III. Electronic Absorption spectra:

The UV-Visible absorption spectra of synthesized ligand and its metal complexes were recorded in DMSO solution at room temperature in 200-800 nm range and the data are presented in Table. The spectra of TFPMMP-SB5 and its all complexes are shown in Figure 1.2 to Figure 1.6. The electronic spectral data of the complexes with all the ligands are presented in Table 1.3
The intense band in the UV region at 303nm for complex copper, 264 nm for nickel complex, 260nm for cobalt complex 257 for Manganese complexis attributed to intra-ligand benzene ring π-π* transition. Another intense band at 400 nm for copper complex, 283 and 309 nm for Ni complex, 410nm for cobalt complex and 361 for Manganese complex is due to the azomethine chromophore n-π* transition of coordinated Schiff base ligands.

Additionally, the copper (II) metal complexes presented a distinct d-d transition band within the visible region, specifically around 570 nm. This spectral feature is attributed to the electronic transition from (2B1g to 2Eg)[14-17]. While square planar copper (II) complexes theoretically allow for three possible d-d transitions, the observed single, broadened band results from the overlapping of these closely spaced transitions. For nickel (II) complexes, two prominent absorption bands were identified at approximately 530 nm and 564 nm. These bands are characteristic of square planar nickel (II) complexes, corresponding to the 1A1g-1A2g and 1A1g-1B1g electronic transitions, respectively. Although three transitions are expected for a square planar geometry, the 1A1g-1E1g transition is effectively masked by a charge transfer (CT) band observed at 408 [18]. The cobalt (II) metal complexes also exhibited a d-d transition band in the visible region, centered around 560 nm. This band is attributed to the electronic transition from 1A1g to 1B1g. The manganese complex displayed a maximum absorption (λmax) at 361 nm, which can be ascribed to a charge transfer transition [19-20]. A distinct ligand-to-metal charge transfer (LMCT) band was also observed at 415 nm. As anticipated for manganese (II) complexes, d-d transitions, being both spin-forbidden and Laporte-forbidden, were not observed in the electronic spectrum. These transitions typically possess such low intensities that they are practically undetectable, rendering them spectroscopically silent[21-22].

Table.1.3: Electronic absorption spectra values for (TFPMMP-SB5) and its metal complexes

S.No	Compound	Transitions in nm
1	TFPMMP-SB5	258 and 300
2	$(TFPMMP\text{-}SB5)_2Cu$	303, 372 and 565
3	$(TFPMMP\text{-}SB5)_2Ni$	264, 302, 403, 585 and 616
4	$(TFPMMP\text{-}SB5)_2Co$	259, 410 and 525
5	$(TFPMMP\text{-}SB5)_2$ $(H_2O)_2$ Mn	257, 460 and 538

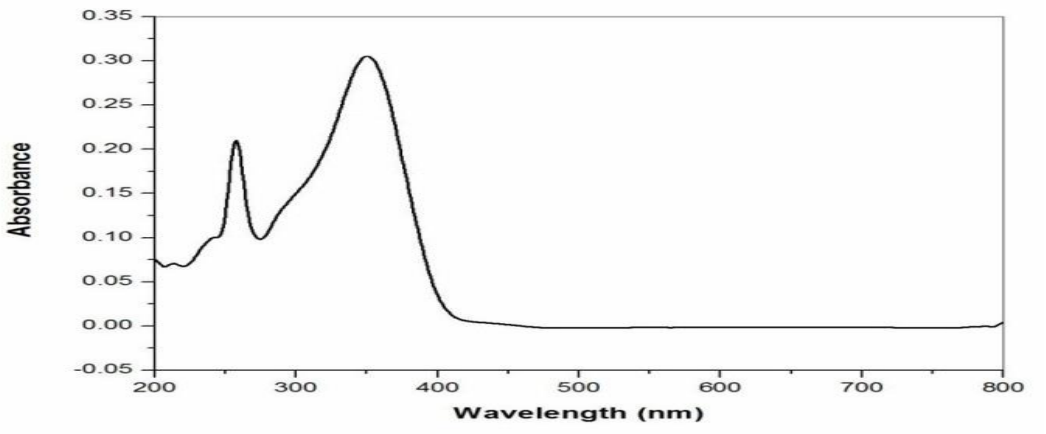

Fig 1.2: UV-Visible spectrum (TFPMMP-SB5)

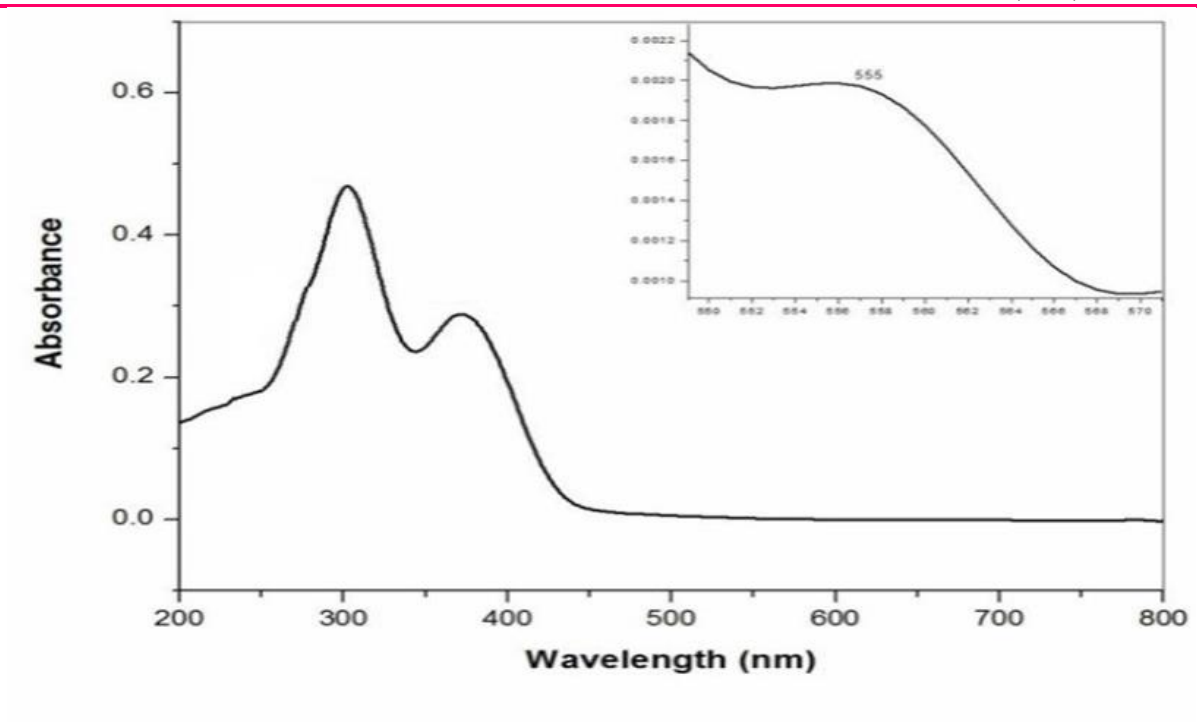

Fig 1.3: UV-Visible spectrum of complex (TFPMMP-SB5)2Cu

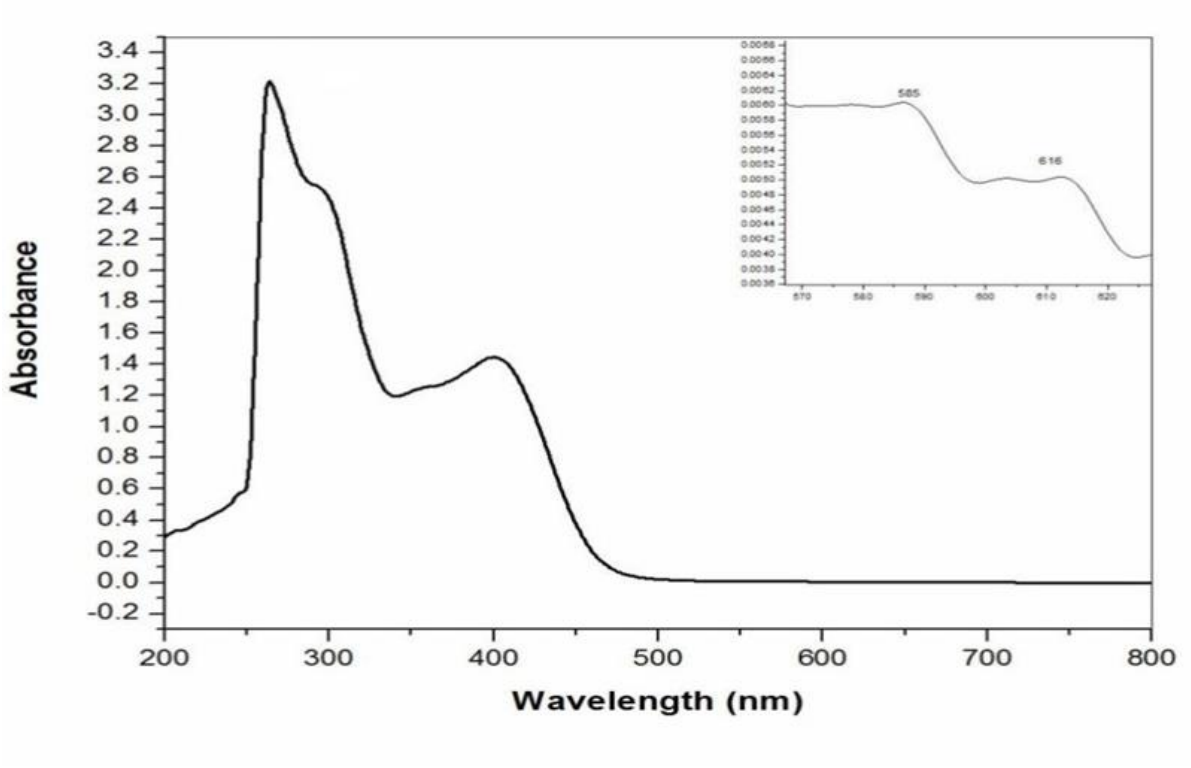

Fig 1.4: UV-Visible spectrum of complex (TFPMMP-SB5)2Ni

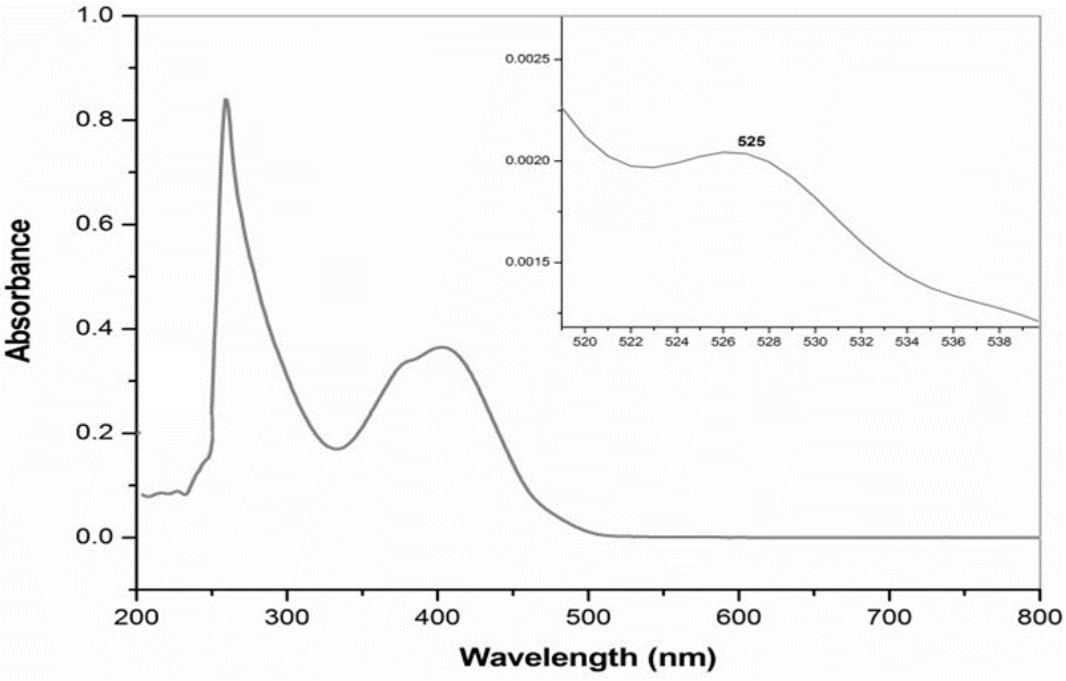

Fig 1.5: UV-Visible spectrum of complex (TFPMMP-SB5)2Co

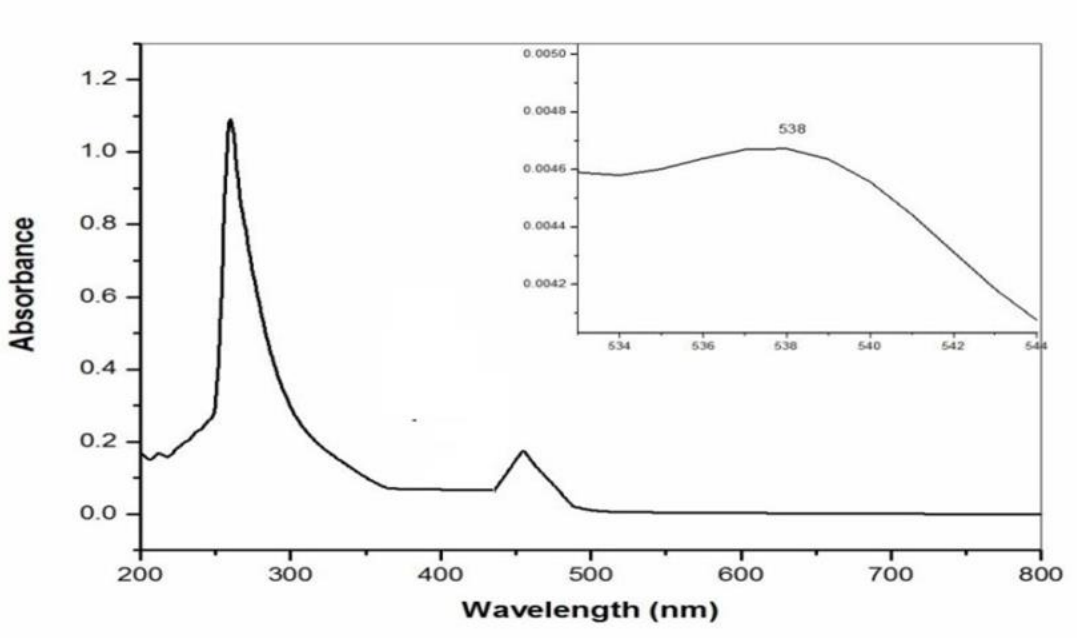

Fig 1.6: UV-Visible spectrum of complex (TFPMMP-SB5)2(H2O)2Mn

IV. IR spectra

The FT-IR spectra of the Schiff base TFPMMP-SB5 and its corresponding metal complexes, recorded within the 5000-400 cm-1 range using KBr discs (as detailed in Table 1.4), exhibit complex profiles characterized by a multitude of bands with varying intensities. Due to this complexity, a complete and unambiguous assignment of all observed bands is challenging. However, based on comparisons with previously reported data in the literature, it is possible to identify and assign some key bands corresponding to important functional groups present in the Schiff base and its complexes.

The Schiff base TFPMMP-SB5 displays a characteristic C=N stretching vibration at 1619 cm-1, indicative of the azomethine function. Upon complexation with metals, this vibration shifts to a lower frequency range of

1600-1606 cm-1. This significant shift in the νC=N stretching frequency of the extranuclear C=N linkage strongly suggests the involvement of the azomethine nitrogen in coordination to the metal. Consequently, the observed bands within the 1600-1606 cm-1 region serve as confirmation of the presence and coordination of the C=N linkage within the resulting metal complexes.

Table 1.4: FT-IR Bands for Schiff Base (TFPMMP-SB5) and its Metal Complexes

S.NO	Compound	ν (O-H)	ν (H_2O)	ν(CH=N)	ν(C-O)	ν (M-O)	ν(M-N)
1	(TFPMMP-SB5)	3432	-	1619	1154	-	-
2	$(TFPMMP-SB5)_2$ Cu	-	-	1600	1190	564	451
3	$(TFPMMP-SB5)_2$Ni	-	-	1605	1180	520	437
4	$(TFPMMP-SB5)_2$Co	-	-	1606	1188	560	425
5	$(TFPMMP-SB5)_2$ Mn	-	3340	1605	1174	565	424

The FT-IR spectra of the metal complexes of the Schiff base exhibit medium to weak intensity bands in the 520-565 cm-1and 436-468 cm-1 regions. These bands are attributed to M-N and M-O stretching vibrations, respectively [23-24]. This confirms that the metal is bonded to the Schiff base through both the azomethine nitrogen and the oxygen atom of the deprotonated –OH group.

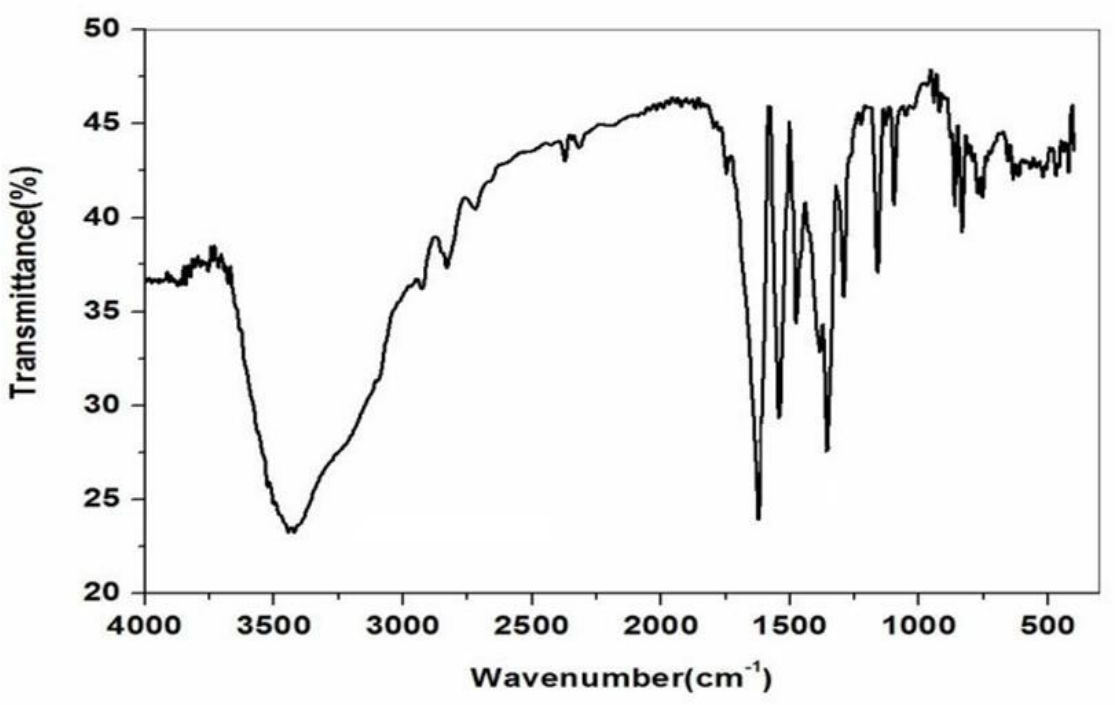

Fig 1.7: IR Spectrum of (TFPMMP-SB5)

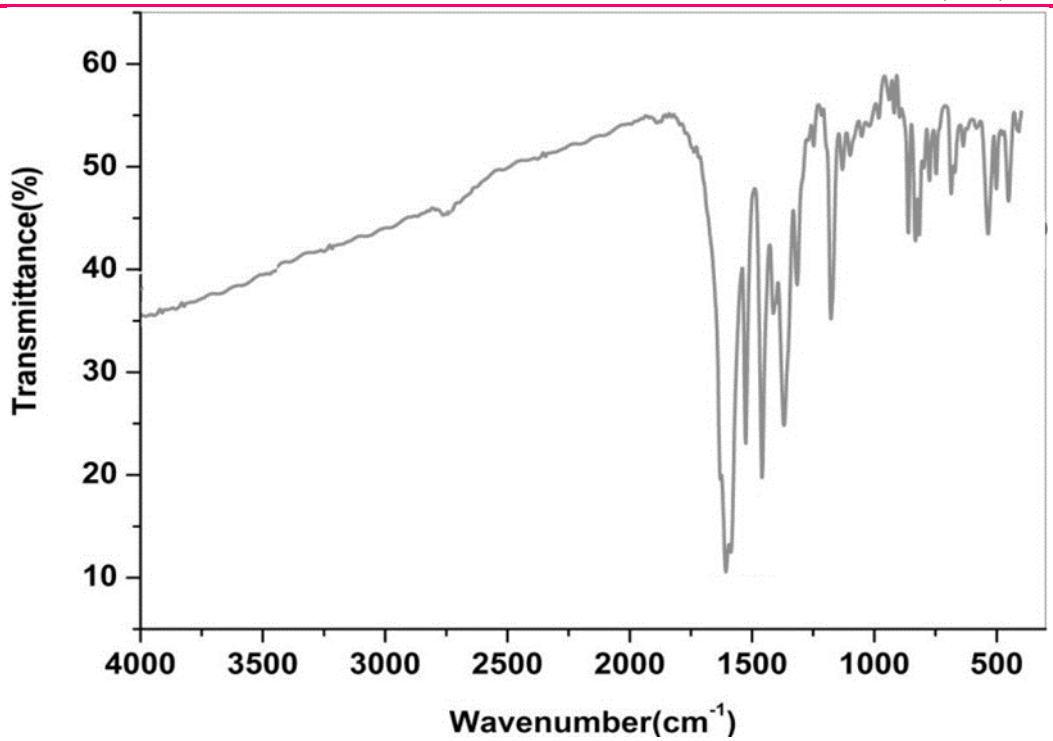

Fig 1.8: IR Spectrum of complex (TFPMMP-SB5)2Cu

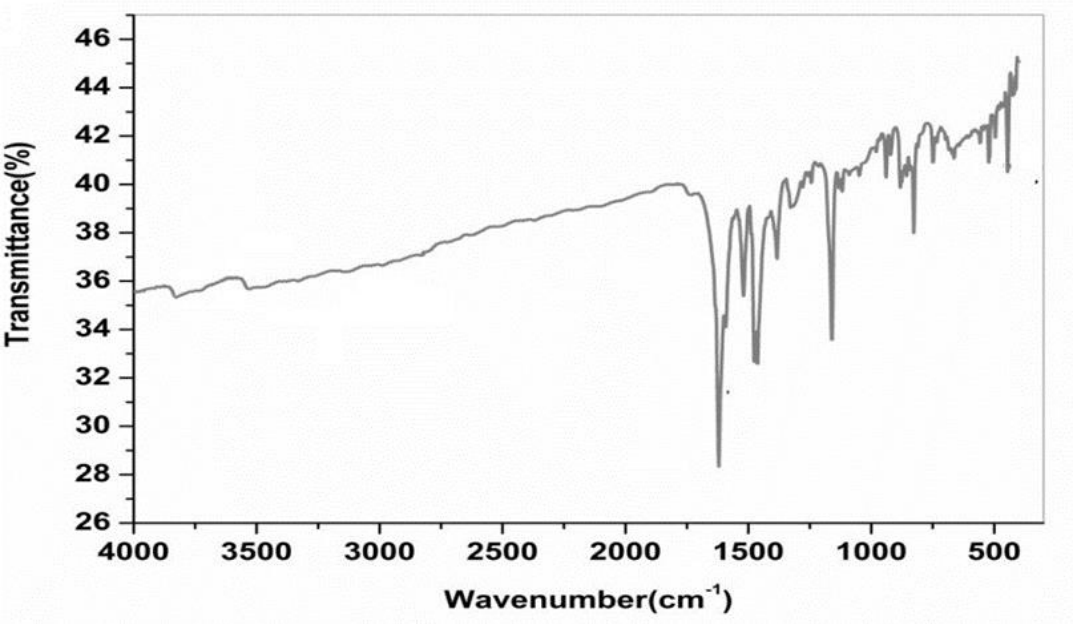

Fig 1.9: IR Spectrum of complex (TFPMMP-SB5)2Ni

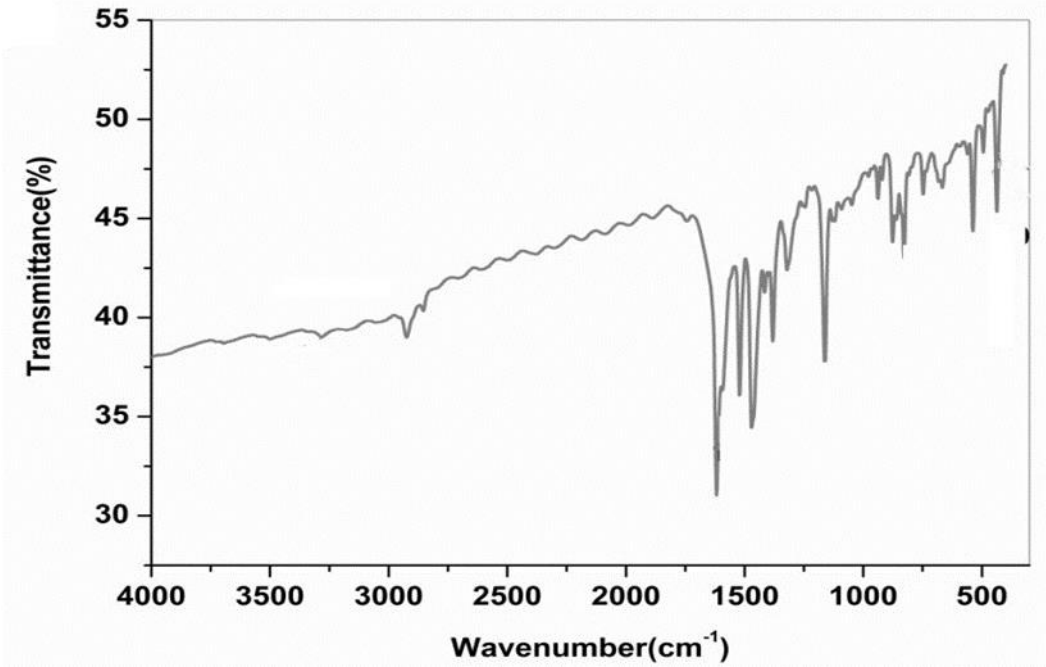

Fig 1.10: IR Spectrum of complex (TFPMMP-SB5)2 Co

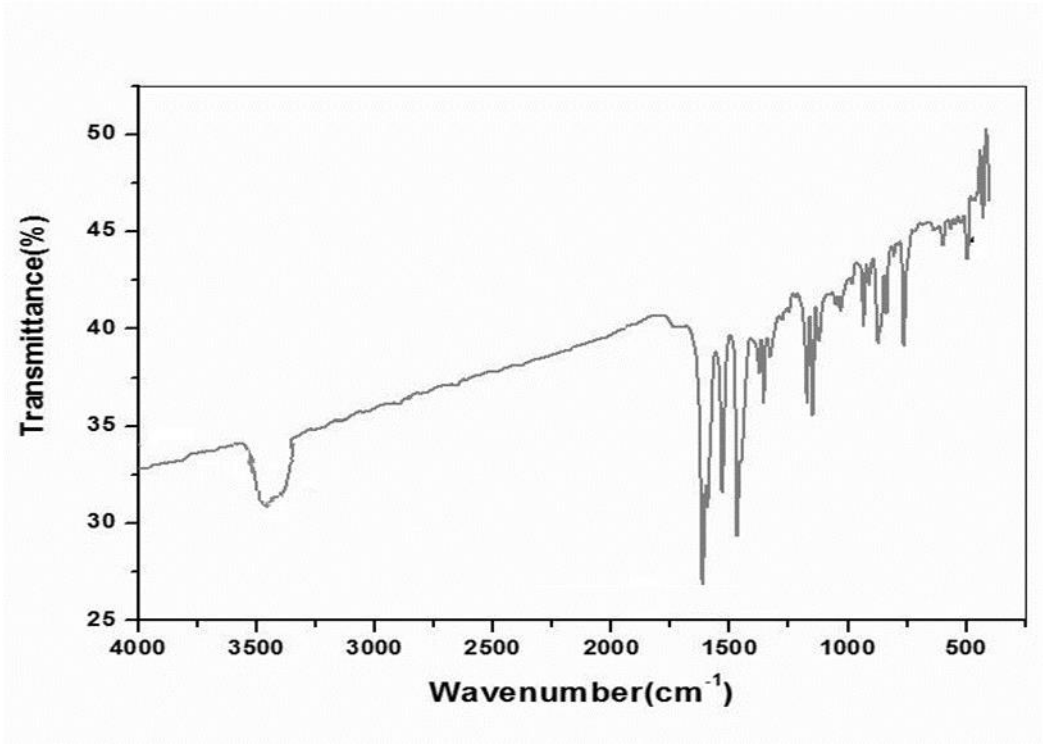

Fig 1.11: IR Spectrum of complex (TFPMMP-SB5)2Mn

V. Thermal analysis

The thermal decomposition behavior of the synthesized metal complexes, as meticulously documented in the Thermogravimetric Analysis (TGA) and Differential Thermal Analysis (DTA) profiles presented in Figures , unveils a consistent two-stage degradation pattern spanning a broad temperature range from 280°C to 855°C. The initial decomposition stage, precisely located within the temperature interval of 280°C to 457°C, is unequivocally attributed to the thermal expulsion of the original ligand moiety initially incorporated into the complex structure. Subsequently, the second decomposition stage, manifesting itself across the temperature range of 440°C to 855°C, corresponds to the complete and thorough volatilization of the remaining organic

components of the ligand, culminating in the formation of a stable metal oxide residue. The observed weight loss profile, as meticulously captured by the TGA curves, finds further corroboration in the presence of distinct endothermic bands within the corresponding DTA curves. These endothermic events precisely align with the temperature regions where the TGA curves register significant weight loss, reinforcing the reliability of the thermal decomposition process interpretation. Notably, the manganese complex exhibited a distinct initial weight loss event between 110°C and 200°C, a characteristic feature attributed to the elimination of coordinated water molecules. This observation strongly suggests the presence of such water molecules within the complex's structural framework. Following this initial dehydration event, a gradual and continuous mass loss was observed up to 300°C, a process likely driven by the progressive decomposition and volatilization of remaining volatile components or ligand fragments. Beyond this critical temperature threshold, the TGA curve plateaued, indicating the formation of a thermally stable metal oxide residue, a testament to the completion of the decomposition process.

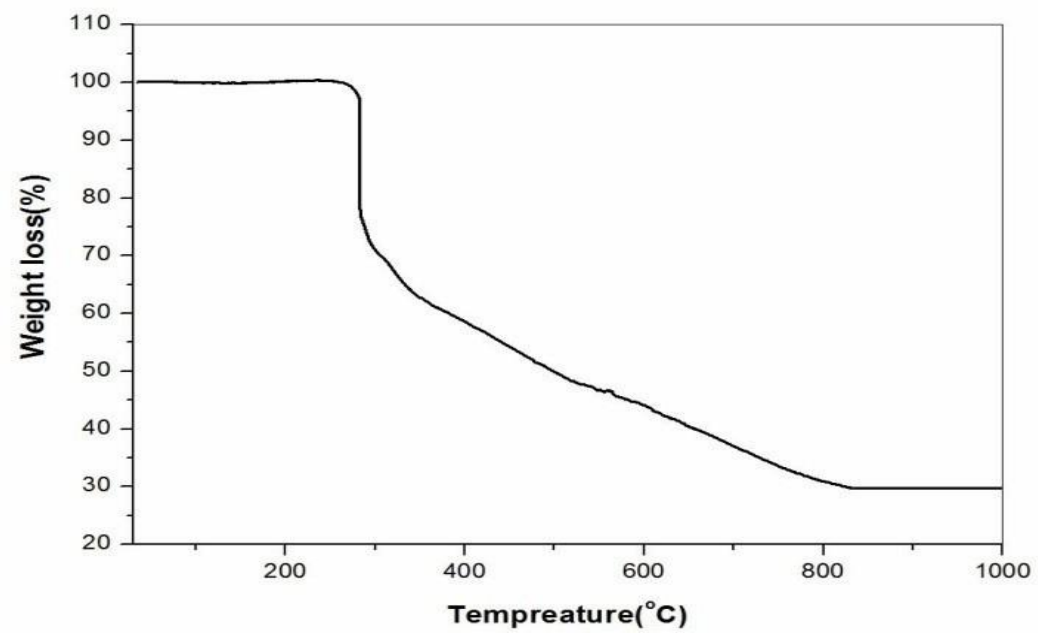

Fig 1.12: TGA & DTA of (TFPMMP-SB5)2Cu.

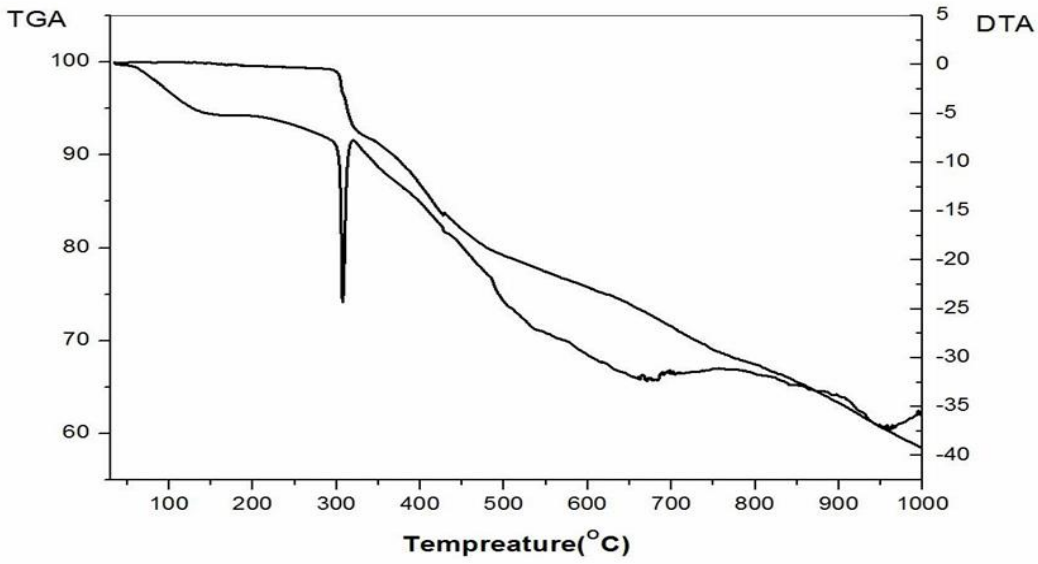

Fig 1.13: TGA & DTA of (TFPMMP-SB5)2 Ni

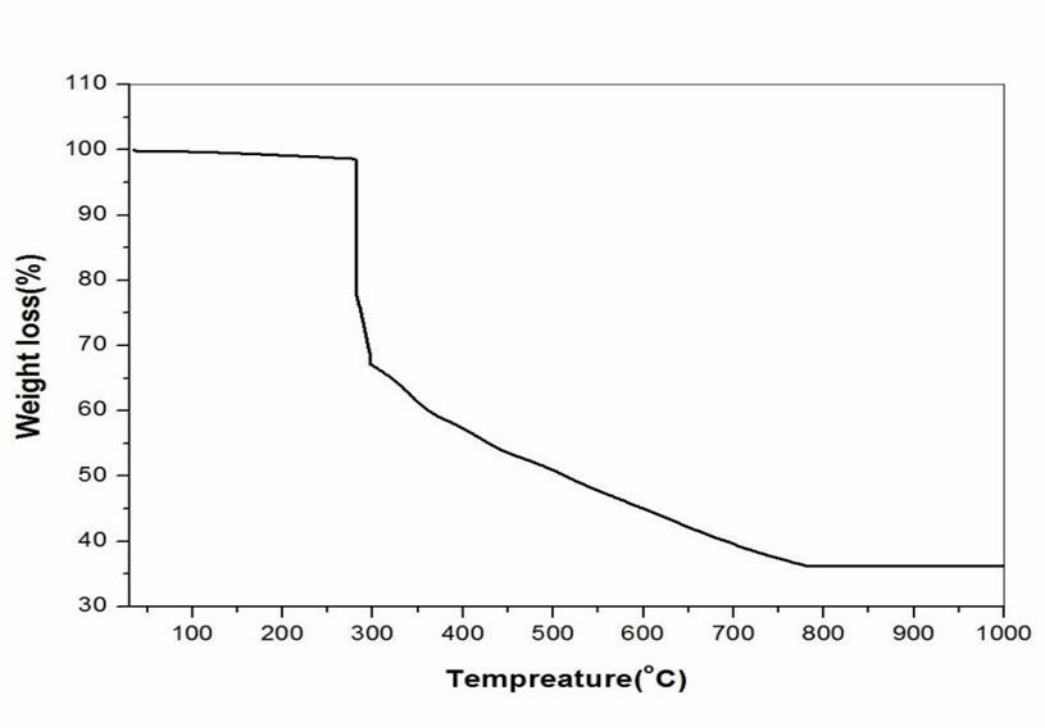

Fig 1.14: TGA & DTA of (TFPMMP-SB5)2Co

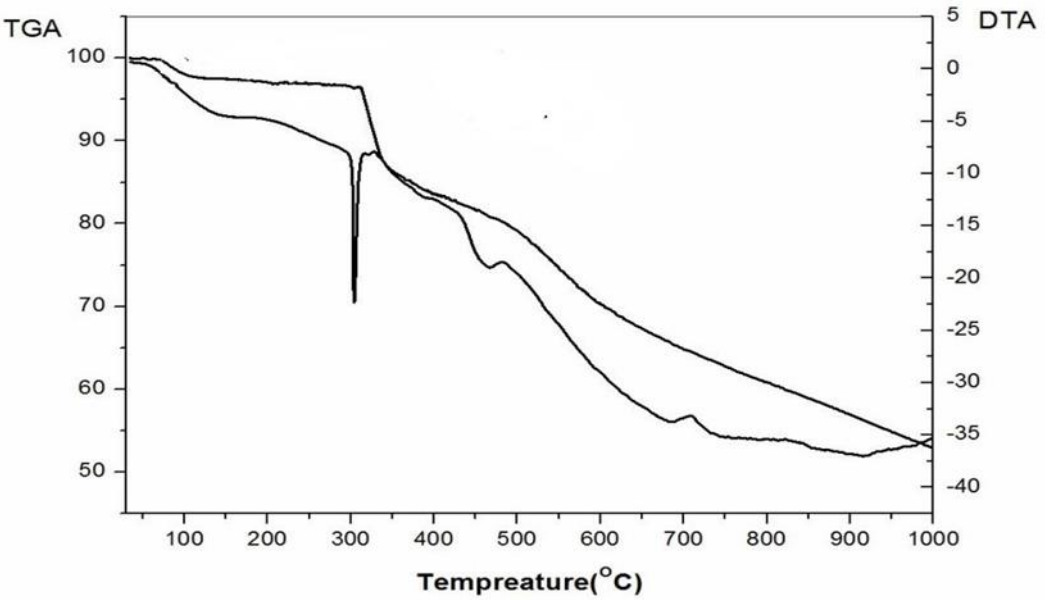

Fig 1.15: TGA & DTA of (TFPMMP-SB5)2Mn

VI. Magnetic moments:

According to Figgis, the magnetic moment values of copper(II) complexes can be indicative of their geometry. He proposed that tetrahedral copper(II) complexes would exhibit magnetic moments exceeding 1.97 B.M, whereas those with square planar and distorted octahedral geometries would have values below this threshold. This distinction arises from the expectation of orbital contribution in the former case and its absence in the latter due to a non-degenerate ground state. Furthermore, square planar and tetragonal complexes generally display magnetic moments slightly higher than the spin-only value of 1.73 B.M, a phenomenon attributed to spin-orbit coupling.

The magnetic moments values of the copper(II) complex calculated in this study at room temperature were slightly higher than the spin-only value, ranging from 1.82 B.M.[25-26]. This observation is indicative of a square planar geometry with one unpaired electron. The small increase in the magnetic moment beyond the spin-only value can be attributed to spin-orbit coupling. Combining the magnetic moment data with electronic spectral and analytical data provides strong evidence for a square planar geometry in the copper(II) complex examined.

The magnetic activity of nickel(II) complex is influenced by their geometry. Complexes with octahedral, square pyramidal or tetrahedral geometries exhibit paramagnetism due to the presence of two unpaired electrons. In contrast, complexes with trigonalbipyramidal or square-planar geometries are diamagnetic, as they have no unpaired electrons.

The magnetic moments of the nickelII) complex examined in this study were found to be diamagnetic. This observation strongly suggests that the nickel(II) complex possess a square planar geometry. This conclusion is further corroborated by evidence from electronic spectra.

Magnetically active cobalt(II) complexes are of two types

Two distinct electronic configurations are considered: i) three unpaired electrons and ii) a single unpaired electron. The former scenario is characteristic of high-spin octahedral and tetrahedral complexes, while the latter is observed in low-spin octahedral and square planar complexes.

Octahedral and tetrahedral cobaltII) complexes typically exist in a high-spin state rather than a low-spin one. High-spin octahedral fields exhibit magnetic moments ranging from 4.7 to 5.2 B.M. These magnetic values result from both spin-only (μ = [4S (S+1)]1/2) and spin plus orbital angular momentum (μ=[4S(S+1)+L(L+1)]1/2). The actual magnetic moment depends on the extent of orbital angular momentum associated with the 4T1g ground state. In square planar complexes, L-S coupling increases the magnetic moment beyond the spin-only value. The Co(II) complex in this study exhibit magnetic moment 2.12 consistent with a square planar geometry. The analyzed Mn(II) complex exhibits a magnetic moment of 5.72, suggesting a high-spin octahedral geometry for the Mn(II) ion. The coordination sphere of the Mn(II) ion likely comprises four oxygen atoms (two from monodentatehydroxy groups of coordinated water molecules and two from Schiff base phenolic groups) and two nitrogen atoms from azomethine groups. However, in the absence of crystallographic data, this interpretation remains speculative, relying solely on magnetic moment values and IR spectral data interpretations.

Magnetic movement of TFPMMP-SB5complexes

Table 1.5: Magnetic moment of (TFPMP-SB5) and its metal complexes

S.No	Complexes	μ_{eff} (BM)
1	$(TFPMMP\text{-}SB5)_2Cu$	1.82
2	$(TFPMMP\text{-}SB5)_2Ni$	0
3	$(TFPMMP\text{-}SB5)_2Co$	2.15
4	$(TFPMMP\text{-}SB5)_2Mn$	5.82

VII. ESR spectroscopy

ESR spectroscopy is a valuable technique for determining the coordination environment of Cu(II) ions. Cu(II) ions exhibit a diverse range of geometries, including tetrahedral, pentacoordinate, hexacoordinate, and various intermediate forms. The geometry of a Cu(II) complex significantly influences the energy levels of its d orbitals, consequently determining the ground state electronic configuration.

Trigonalbipyramidal and compressed octahedral geometries typically result in a d 2 ground state. In contrast, square planar, elongated octahedral and square pyramidal geometries favor a d 2 2ground state.

ESR spectroscopy can effectively differentiate between these ground states by analyzing the 'g' tensor values obtained from anisotropic spectra. These 'g' tensor values provide crucial information about the electronic environment of the unpaired electron in the Cu (II) ion, allowing for the determination of its specific ground

state and, consequently, the geometry of the complex. This version maintains the original length while emphasizing the key aspects of ESR spectroscopy in determining Cu (II) ion environments.

The g value is a critical parameter in electron paramagnetic resonance (EPR) spectroscopy, analogous to the chemical shift in NMR spectroscopy. It signifies the response of a paramagnetic molecule to an external magnetic field. The g value is sensitive to changes in the molecule's electronic structure and provides a quantitative measure of its magnetic moment. For a free electron, the g value is approximately 2.0023. However, in metal complexes, the g value can deviate from this value, either increasing or decreasing.

Shifts in g values arise from spin-orbit coupling. ESR spectroscopy plays a crucial role in enhancing our understanding of copper's physiological significance within copper-containing compounds. The primary objective of ESR studies on copper(II) metal complexes is to elucidate information regarding the order of energy levels, metal-ligand bonding, and unpaired electron distribution. A considerable number of inorganic chemists currently utilize ESR spectroscopic measurements for investigating copper (II) complexes in the solid state.

In most copper (II) complexes, the ground state magnetism primarily arises from spin, with minimal orbital contributions. This is often referred to as "spin-only" magnetism. Since copper(II) ions possess a 3d configuration with a single unpaired electron, the "effective" spin is equivalent to the actual spin of the free ion, S = 1/2. Zeeman splitting, characterized by 'g' factors, deviates from the free electron value of 2.0023 when spin-orbit coupling occurs between the ground and excited states.

In this study, X-band ESR spectra of copper (II) complex was recorded at liquid nitrogen temperature (77 K) using a JES-FA200 ESR spectrometer (JEOL-Japan). Experimental parameters included a 9136.491 MHz microwave frequency, 0.99500 microwave power, and a 100.00 kHz modulation frequency. The corresponding spectra are presented in Figures 1.16.

For square planar complexes, if the unpaired electron is present in the dz2 orbital then the trend follow the order as, g∥>g□>ge(2.0023). While the unpaired electron is present in the dx2– y2 orbital then the trend follows the order as, g∥>g□>ge(2.0023), From the experimental values of copper (II) complexes it is clear that g∥>g□>ge(2.0023). Which provides an evidence of localization of the unpaired electron in dx2–y2 orbital indicating square planar geometry of Cu (II) complexes. The present ESR result for CuII) complex exhibit g∥>g□>ge values below 2.3 indicative of a covalent character in the metal-ligand bond.

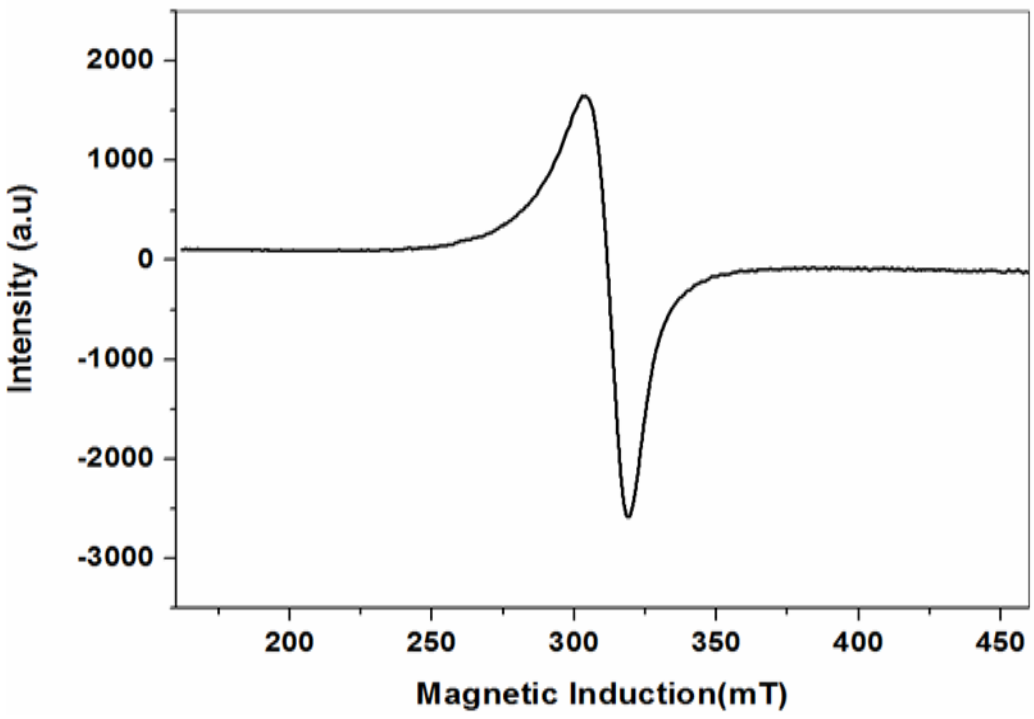

Fig 1.16: ESR Spectrum of (TFPMMP-SB5)2Cu

Table 1.6: ESR Spectral Parameters of (TFPMMP-SB5)2Cu

S.No	Complex	$g_{\parallel}$	$g_{\perp}$	G
1	$(TFPMMP\text{-}SB5)_2Cu$	`2.15	2.09	1.53

Structure of the complexes of (3-(trifluoromethyl)phenyl)imino)methyl)phenol (TFPMMP-SB5)

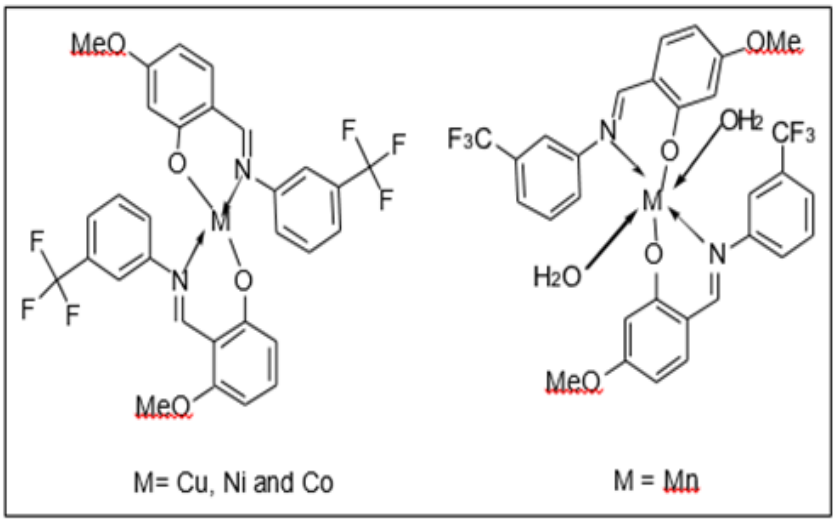

4. Biological activity:

In this study, the antifungal and antibacterial activities were screened for synthesized Schiff bases and their metal complexes. The agar cup method of diffusion was employed for biological screening against Bacillus subtillis, Staphylococcus aureus, Escherichia coli, Klebsiella pneumonia, Aspergillus niger, Aspergillus foetidus, Candida albicans and Candida rogosa utilizing nutrient broth as the culture medium.

1. Media Control: A control containing only sterilized medium is used to ensure the sterility of the medium itself. Growth in this control indicates improper sterilization, invalidating the results.
2. Organism Control: This control consists of sterilized medium inoculated with the test organism. Growth in this control confirms that the medium can support the growth of the organism. If no growth is observed, the medium may be inadequate for the organism's growth.
3. Solvent Control: This control includes sterilized medium, the solvent used to dissolve the test compound, and the test organism. Growth in this control indicates that the amount of solvent used does not inhibit the growth of the organism. If no growth is observed, the solvent may be inhibiting the organism's growth, rendering the test results invalid.

Test sample solutions were prepared at concentrations of 1 mg /1 mL. Subsequently, each solution was added to wells in agar plates inoculated with the desired bacterial and fungal strains. The plates were incubated at 37°C for 48 hours, followed by visual examination for the presence or absence of microbial growth. The results of these studies for Schiff base (TFPMMP-SB5) and its complexes are summarized in the tables below.
Anti-bacterial activity:

Antibacterial screening was performed against Bacillus subtilis, Staphylococcus aureus, Escherichia coli, and Klebsiella pneumoniae to evaluate the activity of a Schiff base and its metal complexes. Ampicillin was used as a positive control and demonstrated intermediate activity, producing inhibition zones of 30 mm against E. coli, 29 mm against K. pneumoniae, 25 mm against B. subtilis, and 28 mm against S. aureus.

Table 1.7: Antibacterial activity of ligand (TFPMMP-SB5) and its metal complexes

Compound	**Bacterial inhibition zone(mm)**			
	Gram-negative bacteria		**Gram-positive bacteria**	
	E.coli	***K.pneumonia***	***S.aureus***	***B.subtilis***
TFPMMP-SB5	10	08	12	10
$(TFPMMP\text{-}SB5)_2Cu$	25	23	20	23
$(TFPMMP\text{-}SB5)_2Ni$	19	17	18	22
$(TFPMMP\text{-}SB5)_2Co$	18	18	19	17
$(TFPMMP\text{-}SB5)_2Mn$	20	21	15	18
Ampicillin	30	29	25	28

I. Antifungal activity of TFPMMP-SB5 and its complexes:

The test compounds were subjected to screening against Aspergillus niger, Aspergillus foetidus, Candida albicans and Candida rugosa using nutrient broth as the culture medium by the agar cup diffusion method. Fluconazole was employed as a standard drug to compare the results.

Table 1.8.Antifungal activity of ligand (TFPMMP-SB5) and its complexes

Compound	**Fungal inhibition zone(mm)**			
	Aspergillus niger	***Aspergillus foetidus***	***Candida albicans***	***Candida rugosa***
TFPMMP-SB5	10	11	09	08
$(TFPMMP\text{-}SB5)_2Cu$	26	22	20	24
$(TFPMMP\text{-}SB5)_2Ni$	15	14	13	22
$(TFPMMP\text{-}SB5)_2Co$	18	17	18	14
$(TFPMMP\text{-}SB5)_2Mn$	16	12	14	16
Fluconazole	29	27	26	30

5. Conclusion:

Antimicrobial activity was assessed by measuring inhibition zone diameters after incubation. Concentrations of the ligand and its metal complexes demonstrated inhibitory effects against E. coli, K. pneumoniae, S. aureus, and B. subtilis, as evident from the data in the table. However, the complexes exhibited higher activity compared to the ligand. The results were compared against ampicillin, which showed intermediate activity. Based on these findings, the synthesized compounds exhibited weak antimicrobial activity against the studied microbes. The order of activity was observed as: Standard antibiotics > Complexes > Ligand and different concentrations of the ligand and its metal complexes demonstrated inhibitory effects against Aspergillus niger, Aspergillus foetidus, Candida albicans, and Candida rugosa, as evident from the zone of inhibition data in the tables. However, the complexes exhibited higher activity compared to the ligand. The results were compared with a standard antifungal agent: Fluconazole, which showed intermediate activity. Based on these findings, the synthesized compounds exhibited weak antimicrobial activity against the studied microbes. The order of activity was observed as: Standard antifungal > Complexes > Ligand.

6. CONFLICTS OF INTEREST

The authors declared no potential conflicts of interest with respect to the research, authorship, and/or publication of this article.

7. PLAGIARISM POLICY

All authors declare that any violation of plagiarism, copyright, or ethical matters is the responsibility of the authors. The journal and its editors bear no liability for such matters.

8. SOURCES OF FUNDING

No external funding was received to carry out this research work. All design and testing work was carried out using facilities at BMS College of Engineering, Bangalore.

References:

[1] E. Colacio, M. Ghazi, M. Kivekas, J.M. Moreno, Inorg. Chem. 39 (2000) 2882.
[2] Q. Hou, L. Zhao, H. Zhang, Y. Wang, S. Jiang, J. Lumin. 126 (2007) 447.
[3] M.R. Ganjali, M.R. Pourjavid, M. Rezapour, T. Poursaberi, A. Daftari, M.S. Niasari, Electroanalysis 16 (2004) 922
[4] R. Antony, S.T. David, K. Saravanan, K. Karuppasamy, S. Balakumar, Spectrochim. Acta. Part A. 103 (2013) 423.
[5] P.G. Lacroix, Eur. J. Inorg. Chem. 2001 (2001) 339.
[6] N. Raman, A. Selvan, S. Sudharsan, Spectrochim. Acta Part A. 79 (2011) 873.
[7] R.Nagane, M. Chikira, M. Oumi, H. Shindo, W.E. Antholine J. Inorg. Biochem.78 (2000) 243.
[8] N.K. Singh, S.B. Singh, Met. Based Drugs.9 (2002) 109.
[9] R. Hernandez-Molina, A. Mederos, J.A. McCleverty, T.J. Meyer, 2005 second ed. Elsevier Science, U.K.
[10] A. Ray, B.K. Seth, U. Pal, S. Basu. Spectrochim.Acta. Part A. 92 (2012) 164.
[11] O.B. Ibrahim, M.A. Mohamed, M.S. Refat. Can. Chem. Trans., 2 (2014) 108.
[12] N. Selvakumaran, N.S.P.Bhuvanesh, A.Endo, R.Karvembu. Polyhedron.,75 (2014)95.
[13] B. Shafaatian, A. Soleymanpour, N.K. Oskouei, B. Notash, S.A. Rezvani. Spectrochim.Acta Part., A. 128 (2014) 363.
[14] Y. Zhou, X.Ye, F. Xin, X. Xin, Transition Met. Chem. 24 (1999) 118.
[15] D.X. West, A.K. El-Sawaf, G.A. Bain, Transit. Met.Chem. 23 (1998) 1.
[16] R. Ramesh, S. Maheswaran, J. Inorg. Biochem.96 (2003) 457.
[17] R.S. Joseyphus, C.J. Dhanaraj, M.S. Nair, Transit. Met.Chem. 31 (2006) 699.
[18] R. Takjoo, R. Centore, A. Akbari, A. Mehdi, Polyhedron. 80 (2014) 243.
[19] A.P. Mishra, S.K. Gautam, J. Indian.Chem. Soc. 81 (2004) 322.
[20] S.A. Carabineiro, L.C. Silva, P.T. Gomes, C.J. Pereira, L.F. Veiros, I. Sofia, M. Pascu, D. Teresa, N. Sónia, R. T. Henriques, Inorg. Chem. 46 (2007) 6880.
[21] Devi, J., Batra, N., and Malhotra, R. (2012). Spectrochim.ActaA Mol. Biomol. Spectrosc. 97, 397–405.
[22] Keypour, H., Shayesteh, M., Rezaeivala, M., Chalabian, F., and Valencia, L. (2013). Spectrochim.ActaA Mol. Biomol. Spectrosc.101, 59–66 (2013).
[23] E. Erdem, E.Y. Sari, R. Kilinçarslan, N. Kabay, Transition Met.Chem. 34 (2009) 167.
[24] L.J. Bellamy, The Infrared Spectra of Complex Molecules, second ed., Chapmann and Hall, London, 1980.
[25] P.P. Dholayika, M.N. Patel, Synth. React. Inorg.Met-Org. Nano-Chem. 34 (2004) 383.
[26] F.A. Cotton, G. Wilkinson, Advanced Inorganic Chemistry, third ed., InterscicencePublisher, New York, 1972